

# Hydrodynamic pressures acting on rigid gravity dams during earthquakes

## Pressions hydrodynamiques s'exerçant sur les barrages poids rigides pendant un tremblement de terre.

YONG-SIK CHO, *Department of Civil Engineering, Hanyang University, 17 Haengdang-dong, Seongdong-gu, Seoul 133-791, Korea, (e-mail) ysc59@hanyang.ac.kr; (fax) 82-2-2293-9977*

PHILIP L.-F. LIU, *School of Civil and Environmental Engineering, Hollister Hall, Cornell University, Ithaca, NY 14853, USA, (e-mail) pll3@cornell.edu*

### ABSTRACT

A boundary integral equation model is developed based on the analytical integrals for three-dimensional potential problems. All necessary integrals are first converted into line integrals around a target element and then integrated analytically. The developed model is applied to a practical problem concerning computation of the hydrodynamic pressure acting on a dam face of a dam-reservoir system during earthquakes. The obtained numerical solutions are compared with available two-dimensional experimental data and analytical solutions. A very good agreement is observed. The model is then used to investigate three-dimensional effects of a complex dam-reservoir system.

### RÉSUMÉ

On développe un modèle d'équations intégrales de frontières, basé sur les intégrales analytiques pour les problèmes potentiels tridimensionnels. Toutes les intégrales nécessaires sont d'abord converties en intégrales curvilignes autour d'un élément cible, puis intégrées analytiquement. Le modèle ainsi développé est appliqué au problème concret du calcul de la pression hydrodynamique qui s'exerce, lors d'un tremblement de terre, sur la face amont d'un barrage avec retenue. Les solutions numériques obtenues sont comparées avec des résultats bidimensionnels expérimentaux et analytiques. On observe un très bon accord. Le modèle est alors utilisé pour étudier les effets tridimensionnels dans un système complexe de barrage avec retenue.

## 1. Introduction

Hydrodynamic pressures acting on gravity dams due to ground motions have been widely and frequently investigated by many researchers because of its important and direct application in designing a dam. Although there are experimental study (e.g. Zangar, 1953), analytical solutions (e.g. Westergaard, 1933; Chwang, 1978; Liu, 1986), approximate analytical solutions (e.g. Aviles and Sanchez-Sesma, 1989) and many numerical models (e.g. Hall and Chopra, 1982; Liu and Cheng, 1984; Humar and Jablonski, 1988) for two-dimensional problems, a three-dimensional application is still rare.

An analytical solution for the hydrodynamic pressure acting on the dam due to earthquake was first obtained by Westergaard (1933). Zangar (1953) performed laboratory experiments and obtained data for the hydrodynamic pressure acting on dams due to horizontal shakings. An electric analog device was used to calculate the hydrodynamic pressure. Zangar's pressure data were compared with Westergaard's analytical solutions for dams with a vertical upstream face.

Chwang and Housner (1978) presented approximated solutions obtained from the momentum balance principle for the hydrodynamic pressure distribution acting on an inclined dam face. It was assumed that the duration of the dam acceleration is short enough so that the compressibility of the fluid is negligible. The reservoir is simplified to have a constant depth and an infinite length. In a companion paper, Chwang (1978) also presented an analytical

solution obtained by using a two-dimensional potential flow theory for the same problem of Chwang and Housner (1978).

Liu (1986) presented analytical solutions for the earthquake-acceleration-induced hydrodynamic pressure on a rigid sloping dam with a triangle-shaped reservoir. Both vertical and horizontal ground motions were taken into consideration. Chwang's (1978) solution can be viewed as a limiting case of Liu's analytical solutions. Liu also investigated the problem with complex geometries of the reservoir numerically using a two-dimensional boundary integral equation method. The obtained numerical solutions were compared with Zangar's (1953) experimental data for several different dam slopes.

Jablonski and Humar (1990) also solved the dam-reservoir problem using a three-dimensional boundary integral equation method. In their boundary integral equation formulation, elements are quadrilateral and constant, that is,  $\Phi$  and  $\partial\Phi/\partial n$  are assumed to be constant over an element. Moreover, all integrals are done by using the Gaussian quadrature method.

Recently, Chen (1994) presented numerical solutions for the nonlinear hydrodynamic pressures acting on dam faces using a two-dimensional finite difference method. The effect of nonlinear convective acceleration is considered. However, the maximum free surface rising near the dam face is small (less than 5% of the still water depth). Chen compared his numerical solutions with Liu's (1986) exact solutions.

In this paper, a numerical model based on a three-dimensional boundary integral equation method is developed and applied to

Revision received February 13, 2001. Open for discussion till August 31, 2002.

computation of the hydrodynamic pressure acting on a dam face of a dam-reservoir system during earthquakes. The dam and bottom and banks of the reservoir are assumed to be rigid in this study. The effects of water compressibility and acoustic radiation from the reservoir bottom are ignored. The accuracy of the present numerical model is verified by comparing numerical solutions with experimental data (Zangar, 1953) and analytical solutions (Liu, 1986) for two-dimensional cases. Three-dimensional effects are also examined.

In the following section, the boundary integral equation is first formulated in brief. The analytical expressions for all necessary integrals are then derived and presented. The governing equation and boundary conditions are described in section 3. Numerical solutions and discussions are given in section 4. Finally, concluding remarks are made in section 5.

## 2. Boundary Integral Equation Method

The boundary integral equation method has been developed as a powerful tool for solving various three-dimensional potential flow problems (e.g. Medina and Liggett, 1988, 1989; Jablonski and Humar, 1990; Cao et al., 1991). All these problems solved an integral equation for a velocity potential function  $\Phi$  in the following form:

$$-\alpha_1 \Phi_P = \int_{\partial D} \left[ \Phi_Q \frac{\partial}{\partial n} \left( \frac{1}{r} \right) - \frac{1}{r} \frac{\partial \Phi_Q}{\partial n} \right] dA \quad (1)$$

where  $r$  is the distance between a base point denoted by the subscript  $P$ , and a field point denoted by the subscript  $Q$ , on the boundary,  $\alpha$  is the solid angle at the point ( $\alpha_1$  takes  $4\pi$  if  $P$  is inside the domain,  $2\pi$  when  $P$  is on a smooth boundary and zero when  $P$  is outside the domain) and  $\partial/\partial n$  denotes the normal derivative on the boundary  $\partial D$ .

The integrals on the right-hand side of equation (1) can be integrated numerically after the boundary is discretized into a finite number of elements and the variation of potential function  $\Phi$  and its normal derivative  $\partial\Phi/\partial n$  is approximated over each element. Numerical integrations can normally provide results with desirable accuracy except for the cases where the integrand is nearly singular, i.e. when  $P$  and  $Q$  are very close to each other. Since they are not singular, the integration can not be performed by special methods for singularity. Therefore, a numerical integration can not always yield accurate result. Some examples for nearly singular problems are given in Medina and Liggett (1989). An alternative is to integrate these integrals analytically. Medina and Liggett (1988) demonstrated that using a linear triangular element with a linear shape function for  $\Phi$  and  $\partial\Phi/\partial n$ , analytical solutions for these integrals can be indeed obtained. Hence, the difficulties with the nearly singular integral can be removed.

A local coordinate system  $(\xi, \zeta, \eta)$  in which the  $\xi - \zeta$  plane is parallel to the element, the  $\eta$ -coordinate is normal to the element and the origin is located at the observation point is shown in Fig.1. The shape functions for  $\Phi$  and  $\partial\Phi/\partial n$  are given as

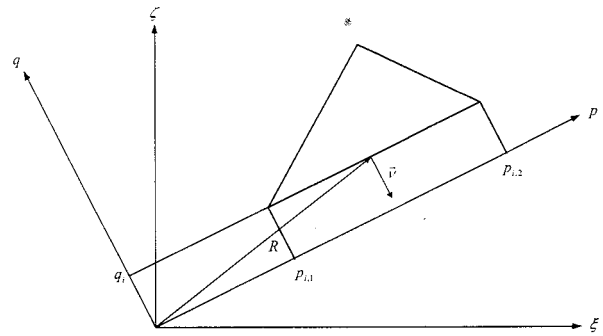


Fig. 1 A triangular element in  $\xi - \zeta$  and  $p - q$  coordinate system

$$\Phi = l_1 \xi + m_1 \zeta + n_1 \quad (2a)$$

$$\frac{\partial \Phi}{\partial n} = l_2 \xi + m_2 \zeta + n_2 \quad (2b)$$

where  $l_1, m_1, n_1, l_2, m_2$  and  $n_2$  are expressed in terms of the potentials and its normal derivatives at the nodes. By substituting equation (2) into equation (1), we can show that the following integrals need to be evaluated

$$\begin{aligned} I_1 &= \int_A \frac{1}{r} dA, \quad I_1^\xi = \int_A \frac{\xi}{r} dA, \quad I_1^\zeta = \int_A \frac{\zeta}{r} dA \\ I_2 &= \int_A \frac{1}{r^3} dA, \quad I_2^\xi = \int_A \frac{\xi}{r^3} dA, \quad I_2^\zeta = \int_A \frac{\zeta}{r^3} dA \end{aligned} \quad (3)$$

In Medina and Liggett (1988), analytical solutions are obtained by two methods:  $I_1$  and  $I_2$  were converted into line integrals around a boundary element, and the rest of integrals were done by area integration. In this paper, we shall show that all integrals given in equation (3) can be integrated as line integrals around the target element. This implies that the three-dimensional potential problem is reduced to a one-dimensional integral equation. Therefore, the present analytical solutions for these integrals are much simpler.

### 2.1 Line Integrals

We shall first show that the area integrals given in equation (3) can be converted to line integrals around a target element by using the divergence theorem and the Green's theorem. The divergence theorem is given as

$$\int_A \nabla^2 V dA = \int_{\partial A} \nabla V \cdot \vec{v} ds \quad (4)$$

where  $V$  is a suitable twice-differentiable function,  $\partial A$  denotes the boundary of the element and  $\vec{v}$  represents the unit normal to the boundary of a triangle.

We begin with the first integral  $I_1$ . To express  $I_1$  in terms of a line

integral, we define

$$\nabla^2 V = \frac{1}{r} = \frac{1}{\sqrt{R^2 + \eta^2}} \quad (5)$$

where

$$R = \sqrt{\xi^2 + \zeta^2} \quad (6)$$

Following Medina and Liggett's (1988) approach, the function  $V$  is obtained by expressing the two-dimensional Laplacian in terms of cylindrical coordinates and retaining only the radial terms

$$\frac{1}{R} \frac{\partial}{\partial R} \left( R \frac{\partial V}{\partial R} \right) = \frac{1}{\sqrt{R^2 + \eta^2}} \quad (7)$$

Integrating equation (7) and excluding the singular solution, we can get

$$V = r - \eta \ln(r + \eta) \quad (8)$$

The integration constant has been fixed as zero without loss of generality. In Medina and Liggett's results, a singular term,  $\eta \ln(R)$ , was included (see equation (34) of Medina and Liggett). The intensity of the singularity was specified arbitrarily. The inclusion of singularity is not wrong but unnecessary. Substituting equation (8) into equation (4), we obtain

$$I_1 = \int_{\partial A} \frac{r}{r + \eta} \frac{\partial r}{\partial v} ds \quad (9)$$

Equations (8) and (9) are also valid, if  $\eta = 0$ . Because the singular solution is not included in equation (8), there is no need to check if the projection of the base point falls on the target element. The integral  $I_2$  is performed in a similar manner. The function  $V$  is the particular solution of

$$\frac{1}{R} \frac{\partial}{\partial R} \left( R \frac{\partial V}{\partial R} \right) = \frac{1}{r^3} = \frac{1}{(R^2 + \eta^2)^{3/2}} \quad (10)$$

Thus, for  $\eta \neq 0$

$$V = \frac{1}{\eta} \ln(r + \eta) \quad (11a)$$

and for  $\eta = 0$

$$V = \frac{1}{R} \quad (11b)$$

Therefore,  $I_2$  becomes

$$I_2 = \int_{\partial A} \frac{1}{\eta(r + \eta)} \frac{\partial r}{\partial v} ds \quad (12a)$$

for  $\eta \neq 0$ , and

$$I_2 = - \int_{\partial A} \frac{1}{R^2} \frac{\partial R}{\partial v} ds \quad (12b)$$

for  $\eta = 0$ .

The area integrals  $I_1^\xi$ ,  $I_1^\zeta$ ,  $I_2^\xi$  and  $I_2^\zeta$  can also be converted to the line integrals using the Green's theorem which can be expressed as (Greenberg, 1978)

$$\int_S \left( \frac{\partial N}{\partial \xi} - \frac{\partial M}{\partial \zeta} \right) d\xi d\zeta = \oint_C (M d\xi + N d\zeta) \quad (13)$$

where  $C$  is a simply closed curve enclosing a simply connected region  $S$ . The direction of integration along  $C$  is counterclockwise. To convert the area integral  $I_1^\xi$  into a line integral, we first note that

$$\frac{\xi}{r} = \frac{\partial r}{\partial \xi} \quad (14)$$

since  $r^2 = \xi^2 + \zeta^2 + \eta^2$ . Using the Green's theorem (13) we convert the integral  $I_1^\xi$  to

$$\begin{aligned} I_1^\xi &= \int_A \frac{\partial r}{\partial \xi} dA \\ &= \oint_C r d\zeta \end{aligned} \quad (15)$$

in which  $M = 0$  and  $N = r$  have been used in the Green's theorem (13). The integral  $I_1^\zeta$  is also done in a similar manner. Because  $\xi$  and  $\zeta$  are independent of each other, the line integral can be obtained from equation (15) by replacing  $\xi$  by  $\zeta$ .

$$\begin{aligned} I_1^\zeta &= \int_A \frac{\partial r}{\partial \zeta} dA \\ &= - \oint_C r d\xi \end{aligned} \quad (16)$$

The integral  $I_2^\xi$  can be written as

$$\begin{aligned} I_2^\xi &= \int_A \frac{\xi}{r^3} dA \\ &= \oint_A \frac{\partial}{\partial \xi} \left( -\frac{1}{r} \right) dA \end{aligned} \quad (17)$$

Applying the Green's theorem (13) with  $M = 0$  and  $N = -1/r$  to equation (17), the integral  $I_2^\xi$  becomes

$$I_2^\xi = - \oint_C \frac{1}{r} d\zeta \quad (18)$$

Similarly, the integral  $I_2^\zeta$  can be expressed as

$$I_2^\zeta = \oint \frac{1}{r} d\zeta \quad (19)$$

## 2.2 Analytical Expressions for Line Integrals

The line integrals given in equations (9), (12) and (15)-(19) are integrated in two ways: equations (9) and (12) are integrated using a local coordinate system,  $(p, q)$  in the plane of the target triangle with  $p$  parallel to the side being integrated (Fig. 1); equations (15)-(19) are integrated using a linear relationship between  $\xi$  and  $\zeta$ .

First, the  $(p, q)$  coordinate system is defined three times for each element; once for each side of the triangle. We also introduce a relationship between  $(\xi, \zeta)$  coordinate system and  $(p, q)$  coordinate system as

$$\xi_i = a_i p_i + b_i q_i \quad (20a)$$

$$\zeta_i = c_i p_i + d_i q_i \quad (20b)$$

where  $a_i, b_i, c_i$  and  $d_i$  ( $i=1, 2, 3$ ) are known constants. Since  $R_i^2 = p_i^2 + q_i^2$  and  $r_i^2 = R_i^2 + \eta^2$ , we have

$$\frac{\partial R_i}{\partial v} = -\frac{q_i}{R_i} \quad (21a)$$

$$\frac{\partial r_i}{\partial v} = -\frac{q_i}{r_i} \quad (21b)$$

Using equation (21) we can integrate the line integrals  $I_1$  and  $I_2$  analytically. The procedure is lengthy but straightforward and will not be shown here; only the results are presented here. Thus, from equation (9)

$$I_1 = -\sum_{i=1}^3 \left[ q_i \ln(p_i + r_i) + \eta \tan^{-1} \left( \frac{\eta p_i}{q_i r_i} \right) - \eta \tan^{-1} \left( \frac{p_i}{q_i} \right) \right]_{p_{i,1}}^{p_{i,2}} \quad (22)$$

where  $p_{i,1}$  and  $p_{i,2}$  represent a beginning and an end points, respectively, for each side of a triangular element in  $(p, q)$  coordinate system. Equation (22) is also valid for  $\eta = 0$ . For the integral  $I_2$  the analytical expression is given by

$$I_2 = \sum_{i=1}^3 \frac{1}{\eta} \left[ \tan^{-1} \left( \frac{\eta p_i}{q_i r_i} \right) - \tan^{-1} \left( \frac{p_i}{q_i} \right) \right]_{p_{i,1}}^{p_{i,2}} \quad (23)$$

for  $\eta \neq 0$ , and

$$I_2 = \sum_{i=1}^3 \left[ \frac{p_i}{q_i R_i} \right]_{p_{i,1}}^{p_{i,2}} \quad (24)$$

for  $\eta = 0$ .

Secondly, the linear relationship between  $\xi$  and  $\zeta$  on each triangular element can be expressed as:

$$\xi_i = A_i \zeta_i + B_i \quad (25a)$$

$$\zeta_i = C_i \xi_i + D_i \quad (25b)$$

where  $A_i, B_i, C_i$  and  $D_i$  ( $i=1, 2, 3$ ) can be found with given  $(\xi, \zeta)$  coordinates. Integration of equation (15) leads to

$$I_1^\xi = \sum_{i=1}^3 \left[ \frac{\sqrt{A_i^2 + 1}}{2} \left\{ \alpha_i \sqrt{\alpha_i^2 + \beta_i^2} + \beta_i^2 \ln \left( \alpha_i + \sqrt{\alpha_i^2 + \beta_i^2} \right) \right\} \right]_{\zeta_{i,1}}^{\zeta_{i,2}}, \quad (26)$$

where

$$\alpha_i = \zeta_i + \frac{A_i B_i}{A_i^2 + 1}, \quad \beta_i = \frac{\sqrt{(A_i^2 + 1)\eta^2 + B_i^2}}{A_i^2 + 1}. \quad (27)$$

The integral  $I_1^\zeta$  takes a similar form to that for  $I_1^\xi$  given in equation (26) except that  $\alpha_i, \beta_i$  and  $A_i$  are replaced by  $\gamma_i, \delta_i$  and  $C_i$ , respectively. Thus, the integral  $I_1^\zeta$  is given as

$$I_1^\zeta = -\sum_{i=1}^3 \left[ \frac{\sqrt{C_i^2 + 1}}{2} \left\{ \gamma_i \sqrt{\gamma_i^2 + \delta_i^2} + \delta_i^2 \ln \left( \gamma_i + \sqrt{\gamma_i^2 + \delta_i^2} \right) \right\} \right]_{\xi_{i,1}}^{\xi_{i,2}}, \quad (28)$$

where

$$\gamma_i = \xi_i + \frac{C_i D_i}{C_i^2 + 1}, \quad \delta_i = \frac{\sqrt{(C_i^2 + 1)\eta^2 + D_i^2}}{C_i^2 + 1} \quad (29)$$

In equations (26) and (28),  $(\zeta_{i,1}, \zeta_{i,2})$  and  $(\xi_{i,1}, \xi_{i,2})$  also represent a set of beginning and end points, respectively, for each side of a triangular element in  $(\xi, \zeta)$  coordinate system.

For the integral  $I_2^\xi$ , equation (18) can be integrated analytically to give

$$I_2^\xi = -\sum_{i=1}^3 \left[ \frac{1}{\sqrt{A_i^2 + 1}} \ln \left( \alpha_i + \sqrt{\alpha_i^2 + \beta_i^2} \right) \right]_{\zeta_{i,1}}^{\zeta_{i,2}} \quad (30)$$

Similarly,  $I_2^\zeta$  becomes

$$I_2^\zeta = \sum_{i=1}^3 \left[ \frac{1}{\sqrt{C_i^2 + 1}} \ln \left( \gamma_i + \sqrt{\gamma_i^2 + \delta_i^2} \right) \right]_{\xi_{i,1}}^{\xi_{i,2}} \quad (31)$$

It is noted that equations (26), (28), (30) and (31) are also valid for  $\eta = 0$ . The procedure of analytical integration is lengthy but final expressions of integrals are simple. Furthermore, these integrals can be easily coded in the computer program.

### 3. Governing Equation and Boundary Conditions

In this section, the developed numerical model is applied to the computation of the hydrodynamic pressure acting on dam-reservoir system subjected to earthquakes. The model is a simplified three-dimensional dam-reservoir system as shown in Fig. 2. The fluid impounded by the dam is assumed to be incompressible and inviscid. And the dam, bottom and banks are also assumed to be rigid. Then, the hydrodynamic pressure satisfies the Laplace equation (Liu, 1986)

$$\nabla^2 P(x, y, z) = 0 \quad (32)$$

If the duration of the acceleration is short enough, the free surface movement can be negligible. The only free surface boundary condition is

$$P(x, y, z) = 0 \quad \text{at} \quad z = h \quad (33)$$

The other boundary conditions can be prescribed as

$$\frac{\partial P}{\partial n_d} = -\rho \bar{a} \cdot \bar{n}_d \quad \text{on} \quad \Gamma_d \quad (34)$$

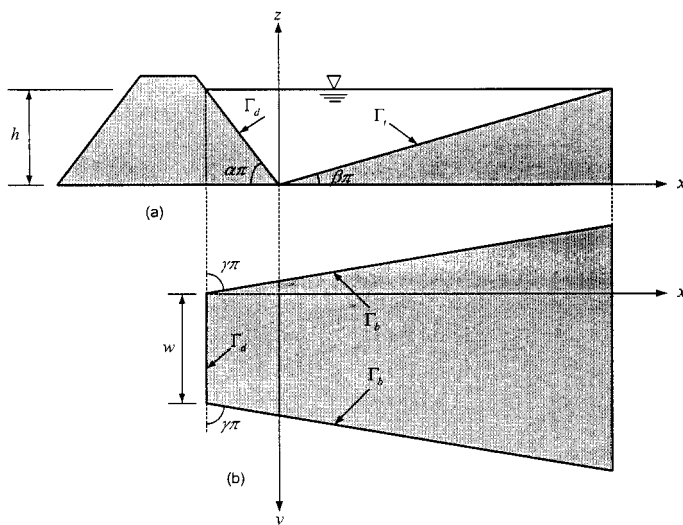


Fig. 2 A simplified dam-reservoir system: (a) cross-sectional view, (b) plan view

$$\frac{\partial P}{\partial n_b} = -\rho \bar{a} \cdot \bar{n}_b \quad \text{on} \quad \Gamma_b \quad (35)$$

$$\frac{\partial P}{\partial n_t} = -\rho \bar{a} \cdot \bar{n}_t \quad \text{on} \quad \Gamma_t \quad (36)$$

in which  $\bar{a}$  is a constant acceleration acting on the dam-reservoir system,  $\rho$  is the density of the fluid, and  $\bar{n}_d, \bar{n}_b$  and  $\bar{n}_t$  are the unit outward normal vectors along the dam face, banks and bottom, respectively.

### 4. Numerical Solutions and Discussion

In numerical computations, the width of dam is taken as the same of the water depth and the fictitious boundary is established at  $x = 6h$  for the infinite reservoir case, i.e. when  $\beta\pi = 0^\circ$ . The detailed description for the fictitious boundary can be found in Liu (1986) and Jablonski and Humar (1990).

The developed model is first applied to the case of  $\gamma\pi = 90^\circ$  and obtained numerical solutions are compared with existing two-dimensional laboratory experimental data (Zangar, 1953) and analytical solutions (Liu, 1986). The model is then applied to other three-dimensional problems.

In Fig. 3, the numerical solutions are compared with the laboratory experimental data and analytical solutions for different dam slopes ( $\alpha\pi$ ) with  $\beta\pi = 0^\circ$  and  $\gamma\pi = 90^\circ$ . If  $\alpha\pi = 90^\circ$ , the upstream dam face becomes vertical. The agreement between the numerical results and analytical solutions is very good, while the experimental data seem to underestimate slightly the hydrodynamic pressures near the bottom in the cases of  $\alpha\pi = 30^\circ$  and  $90^\circ$ . In general, the pressure increases as the dam slope increases. The maximum hydrodynamic pressure occurs at the base of the dam at  $\alpha\pi = 90^\circ$  while it occurs  $z/h \approx 0.2$  for other  $\alpha\pi$  values.

Fig. 4 also shows a comparison between the present numerical results and analytical solutions for  $\beta\pi = 30^\circ$  and  $\gamma\pi = 90^\circ$ . The agreement is also excellent except for  $\alpha\pi = 90^\circ$  where the present

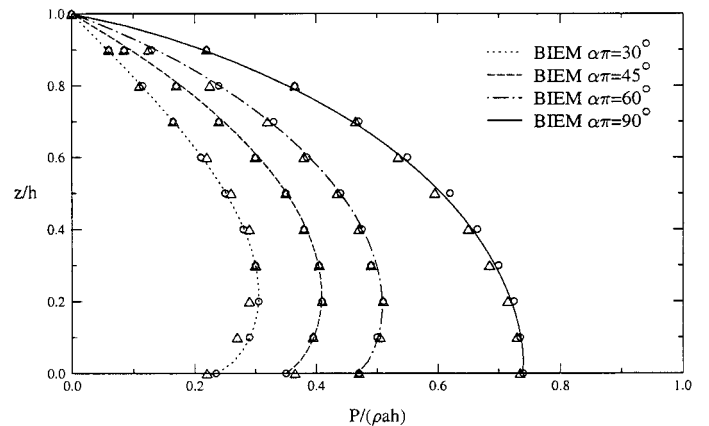


Fig. 3 Pressure distribution on the upstream damface for different bottom slopes ( $\beta\pi = 0^\circ, \gamma\pi = 90^\circ$ ):  $\Delta\Delta\Delta$ , experimental data (Zangar, 1953);  $OOO$ , analytical solutions (Liu, 1986)

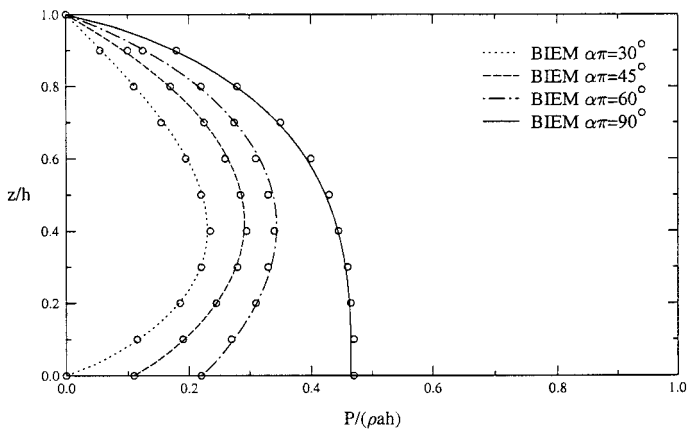


Fig. 4 Pressure distribution on the upstream damface for different bottom slopes ( $\beta\pi = 30^\circ$ ,  $\gamma\pi = 90^\circ$ ): OOO, analytical solutions (Liu,1986)

model seems to overestimate slightly near the bottom. Similarly to Fig. 3, the maximum pressure occurs at the base of the dam when the upstream slope is vertical.

A comparison is made for the case of  $\beta\pi = 45^\circ$  and  $\gamma\pi = 90^\circ$  in Fig. 5. A negative hydrodynamic pressure appears near the base of the dam when  $\alpha\pi = 30^\circ$ . This negative pressure could create cavitation (Liu, 1986) that may cause a severe damage to the dam. Generally, the numerical solutions agree very well with experimental data and analytical solutions.

The numerical model is finally applied to more complex geometries. Fig. 6 shows the calculated hydrodynamic pressures for the cases of  $\alpha\pi = 90^\circ$  and  $\beta\pi = 45^\circ$  with  $\gamma\pi = 15^\circ, 45^\circ, 75^\circ$  and  $90^\circ$ . Since the dam slope is fixed at  $\alpha\pi = 90^\circ$ , the maximum hydrodynamic pressure occurs at the base of the dam for all cases. The pressure becomes larger as  $\gamma\pi$  (bank slope) decreases because more dam face is subjected to earthquake.

## 5. Concluding Remarks

A three-dimensional boundary integral equation model based on the analytical integrals has been developed and used to compute the hydrodynamic pressures acting on rigid dam faces. All neces-

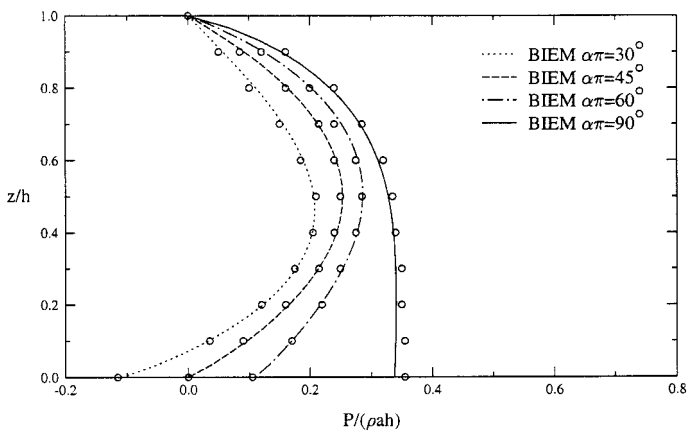


Fig. 5 Pressure distribution on the upstream damface for different bottom slopes ( $\beta\pi = 45^\circ$ ,  $\gamma\pi = 90^\circ$ ): OOO, analytical solutions (Liu,1986)

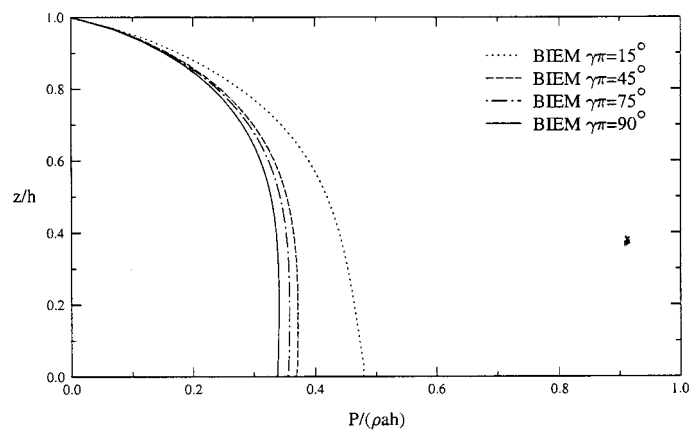


Fig. 6 Pressure distribution on the upstream damface for different bottom slopes ( $\alpha\pi = 90^\circ$ ,  $\beta\pi = 45^\circ$ )

sary integrals are done analytically. The numerical model is first verified by comparing numerical solutions with two-dimensional experimental data and analytical solutions. The agreement between numerical results and experimental data and analytical solutions is very good. The model is then used to study three-dimensional effects of a dam-reservoir system. The developed model can also be applied to other three-dimensional problems as long as the governing equation is the Laplace equation.

## Acknowledgements

The work presented in this paper was supported by Research Funds of the National Research Laboratory Program from the Ministry of Science and Technology in Korea (Costal Engineering Laboratory).

## References

1. AVILES, J. and SANCHEZ-SESMA, F. J., 1989. 'Water pressures on the rigid gravity dams with finite reservoir during earthquakes,' *Earthquake Engineering and Structure Dynamics*, **18**, pp. 527-537.
2. CAO, Y., SCHULTZ, W. W. and BECK, R. F., 1991. 'Three-dimensional desingularized boundary integral methods for potential problems,' *Int. J. for Numerical Methods in Fluids*, **12**, pp. 785-803.
3. CHEN, B.-F., 1994. 'Nonlinear hydrodynamic pressures by earthquakes on dam faces with arbitrary reservoir shapes,' *J. of Hydraulic Research*, **32**, pp. 401-413.
4. CHWANG, A. T., 1978. 'Hydrodynamic pressures on sloping dams during earthquakes. Part 2. Exact theory,' *J. Fluid Mechanics*, **87**, pp.343-348.
5. CHWANG, A. T. and HOUSNER, G. W., 1978. 'Hydrodynamic pressures on sloping dams during earthquakes. Part 1. Momentum method,' *J. Fluid Mechanics*, **87**, pp. 335-341.
6. GREENBERG, M. D., 1978. *Foundations of applied mathematics*, Prentice-Hall Inc., N. J.
7. HALL, J. F. and CHOPRA, A. K., 1982. 'Two-dimensional dynamic analysis of concrete gravity and embankment dams including hydrodynamic effects,' *Earthquake Engineering*

- and *Structure Dynamics*, **10**, pp. 305-332.
8. HUMAR, J. L. and JABLONSKI, A. M., 1988. 'Boundary element reservoir model seismic analysis of gravity dams,' *Earthquake Engineering and Structure Dynamics*, **16**, pp. 1,129-1,156.
  9. JABLONSKI, A. M. and HUMAR, J. L., 1990. 'Three-dimensional boundary element reservoir model seismic analysis of arch and gravity dams,' *Earthquake Engineering and Structure Dynamics*, **19**, pp. 359-376.
  10. LIU, P. L.-F., 1986. 'Hydrodynamic pressures on rigid dams during earthquakes,' *J. Fluid Mechanics*, **165**, pp. 131-145.
  11. LIU, P. L.-F. and CHENG, A. H.-D., 1984. 'Boundary solutions for fluid-structure interaction,' *J. of Hydraulic Engineering*, ASCE, **110**, pp. 51-64.
  12. MEDINA, D. E. and LIGGETT, J. A., 1988. 'Three-dimensional boundary element computation of potential flow in fractured rock,' *Int. J. for Numerical Methods in Engineering*, **26**, pp. 2,319-2,330.
  13. MEDINA, D. E. and LIGGETT, J. A., 1989. 'Exact integrals for three-dimensional boundary element potential flow problem,' *Communications in Applied Numerical Methods*, **5**, pp. 555-561.
  14. WESTERGAARD, H. M. 'Water pressures on dams during earthquakes,' *Transactions of ASCE*, **98**, pp. 418-433.

15. ZANGAR, C. N., 1953. 'Hydrodynamic pressures on dams due to horizontal earthquakes,' *Proceedings of Society of Experimental Stress Analysis*, **10**, pp. 93-102.

#### Notations

$\vec{a}$	a constant acceleration acting on the dam-reservoir system
$\partial A$	A boundary of the element
$C$	A closed curve
$h$	A still water depth
$\vec{n}_d, \vec{n}_b, \vec{n}_t$	unit outward normal vectors
$r$	the distance between a base point and a field point
$S$	A connected region
$V$	A suitable twice-differentiable function
$\alpha$	the angle of a dam slope
$\alpha_1$	the solid angle at a point
$\beta$	the angle of a reservoir bottom
$\gamma$	the angle of a dam bank
$\vec{v}$	unit normal to the boundary of a triangle
$\rho$	A density of the fluid
$\Phi$	A potential function
$(\xi, \zeta, \eta)$	A local coordinate system